Heat Transfer in Horizontal Annulus Saturated with Copper Nanofluid under Various Boundary Conditions

Manal Hadi Saleh [1], Amina H. Dhaef [2]

[1]Baghdad University, College of Engineering, Mechanical Department, Jadryia, Baghdad University, Mechanical Department, Iraq

[2]Wasit University, College of Engineering, Mechanical Department, Wasit University, Mechanical Department, Iraq

Abstract: *The natural convection heat transfer of laminar nanofluid flow is investigated numerically taking copper as nano particles and the water as based fluid in a three dimensional annulus enclosure filled with porous media between two horizontal concentric cylinders. 12 annular fins of 3mm length and 2.4 mm thickness attached to the inner cylinder under steady state condition and different wall temperature boundary conditions. The governing equations used Darcy law and Boussinesq's approximation is transformed to dimensionless equations, then the finite difference approach is used to obtain the results using the MATLAB. The parameters affected on the system are modified Rayleigh number (10 $\leq Ra^* \leq$ 500), the copper volume fraction $\left(0 \leq \varphi \leq 0.3\right)$ and for the sinusoidal temperature boundary condition, the parameters are the dimensionless amplitude $\left(0 \leq a \leq 0.8\right)$, the constant dimensionless time $\tau' = 0.2$ and dimensionless period η' (0.005 – 0.05). The results show that For $Ra^* = 500$; adding Cu nanoparticles with $\varphi = 0.3$ cause 268.18% enhancement in heat transfer and For $Ra^* = 500$; adding Cu nanoparticles with $\varphi = 0.3$ cause 268.18% enhancement in heat transfer and applying sinusoidal temperature boundary condition causes 1.7% increase in heat transfer than that of constant wall temperature. A correlation for Nu in terms of Ra^*, volume fraction (φ) and amplitude (a) has been developed.*

Keywords: Laminar Flow, Natural Convection, Nanofluid, Porous Media, Sinusoidal Temperature..

1. Introduction

Coupled heat and mass transfer driven by buoyancy due to temperature and concentration variations in fluid-saturated porous media has been of growing interest during the last several decades because of its great practical applications in modern industry, such as the design of building components for energy consideration, control of pollutant spread in groundwater, compact heat exchangers, solar power collectors and food industries [1]. For the first time [2] investigated the buoyancy driven flows in a square enclosure with periodic heat flux and examined the effects of oscillation frequency of heat generation on natural convection. Other researchers carried out similar studies by considering a clear base fluid within the enclosure as in [3] and [4]. [5] Showed that introducing nanofluids containing nanoparticles with substantially higher thermal conductivities improves the heat transfer performance. The results of this study have also been confirmed by other researchers [6], [7] and [8]. [9] Studied numerically laminar conjugate heat transfer by natural convection and conduction in a vertical annulus formed between an inner heat generating solid circular cylinder and an outer isothermal cylindrical boundary. It is assumed that the two sealed ends of the tube to be adiabatic. The governing equations have been solved using the finite volume approach, using SIMPLE algorithm on the collocated arrangement.

[10] Examined the periodic natural convection in an enclosure filled with nanofluids. Whilst a heat source with oscillating heat flux is located on the left wall of the enclosure, the right wall is maintained at a relatively low temperature and the other walls are thermally insulated. The utilization of nanoparticles, in particular Cu, enhances the heat transfer especially at low Rayleigh numbers. In addition, the oscillation period of heat generation affects the maximum operational temperature of the heat source.

[11] Investigated numerically Natural convection fluid flow and heat transfer inside C-shaped enclosures filled with Cu-Water nanofluid using finite volume method and SIMPLER algorithm. It was found from the obtained results that the mean Nusselt number increased with increase in Rayleigh number and volume fraction of Cu nanoparticles regardless aspect ratio of the enclosure. Moreover the obtained results showed that the rate of heat transfer increased with decreasing the aspect ratio of the cavity. Also it was found that the rate of heat transfer increased with increase in nanoparticles volume fraction.

[12] Analyzed the heat transfer and fluid flow of natural convection in a cavity filled with Al_2O_3/ water nanofluid that operates under differentially heated walls. The heat transfer rates are examined for parameters of non-uniform nanoparticle size, mean nanoparticle diameter, nanoparticle volume fraction, Prandtl number, and Grashof number.

Heat transfer and fluid flow due to buoyancy forces in a partially heated enclosure using nanofluids is carried out by [13] using different types of nanoparticles. The flush mounted heater is located to the left vertical wall with a finite length. The temperature of the right vertical wall is lower than that of heater while other walls are insulated. The finite volume technique is used to solve the governing equations.

[14] Investigated the heat transfer performance in an enclosure including nanofluids with a localized heat source. The hydrodynamics and thermal fields are coupled together using the Boussinesq's approximation.

2. Objective of Research

In the present study, the heat transfer by natural convection of nanofluid taking copper as nano particles and the water as based fluid in a three dimensional annulus enclosure filled with porous media between two horizontal concentric cylinders under steady state condition and for thermal boundary condition of two cases constant or sinusoidal temperature oscillation at the wall of the inner cylinder and for modified Rayleigh number ($10 \leq Ra^* \leq 500$) and the volume fraction $(0 \leq \varphi \leq 0.3)$.

3. Mathematical Model

The effective thermal conductivity of the nano-fluid is approximated by Maxwell-Garnetts model:

$$\frac{k_{nf}}{k_f} = \frac{k_s + 2k_f - 2\varphi\left(k_f - k_s\right)}{k_s + 2k_f + \varphi\left(k_f - k_s\right)} \tag{1}$$

The use of this equation is restricted to spherical nano-particles where it does not account for other shapes of nano-particles. This model is found to be appropriate for studying heat transfer enhancement using nanofluid [9] and [15]

The thermo-physical properties of pure water and nanoparticles are given in **Table 1** [10].

Table 1: Thermo-physical properties of pure fluid and nanoparticles.

physical properties	Pure water	Cu
P(kg/m^3)	997.1	8933
Cp(J/kg K)	4179	385
K(W/m K)	0.613	400
B(1/K)	21x10^{-5}	1.67x10^{-5}

The viscosity of the nanofluid can be approximated as viscosity of a base fluid μ_f containing dilute suspension of fine spherical particles and is given by [16]:

$$\mu_{nf} = \frac{\mu_f}{\left(1-\varphi\right)^{2.5}} \tag{2}$$

The governing equations used are continuity, momentum and energy equations which are transformed to dimensionless equations and the vector potential equation was obtained in the dimensionless form as [17] and [18]:

$$\frac{\partial U_r}{\partial R} + \frac{U_r}{R} + \frac{1}{R}\frac{\partial U_\phi}{\partial \phi} + \frac{\partial U_z}{\partial Z} = 0 \tag{3}$$

$$Ra^* \Pr * C_1 *\left(\sin\phi\ \frac{\partial\theta}{\partial Z}\right) = -\frac{\partial^2\psi_r}{\partial R^2} - \frac{1}{R^2}\frac{\partial\left(R\psi_r\right)}{\partial R} - \frac{2}{R}\frac{\partial\psi_r}{\partial R} - \frac{1}{R^2}\frac{\partial^2\psi_r}{\partial\phi^2} \tag{4}$$
$$- \frac{\partial^2\psi_r}{\partial Z^2} - \frac{2}{R}\frac{\partial\psi_z}{\partial Z}$$

$$Ra^* \Pr\ C_1 *\left(\cos\phi\ \frac{\partial\theta}{\partial Z}\right) = -\frac{\partial^2\psi_\phi}{\partial Z^2} - \frac{\partial^2\psi_\phi}{\partial R^2} - \frac{1}{R^2}\frac{\partial^2\psi_\phi}{\partial\phi^2} \tag{5}$$
$$- \frac{2}{R^2}\frac{\partial\psi_r}{\partial\phi} + \frac{\psi_\phi}{R^2} - \frac{1}{R}\frac{\partial\psi_\phi}{\partial R}$$

$$-\frac{Ra^* \Pr\ C_1}{\alpha_{nf}}\left(\frac{1}{R}\cos\phi\frac{\partial\theta}{\partial\phi} + \sin\phi\frac{\partial\theta}{\partial R}\right) = -\frac{\partial^2\psi_z}{\partial R^2} - \frac{1}{R}\frac{\partial\psi_z}{\partial R} \tag{6}$$
$$- \frac{1}{R^2}\frac{\partial^2\psi_z}{\partial\phi^2} - \frac{\partial^2\psi_z}{\partial Z^2}$$

Where

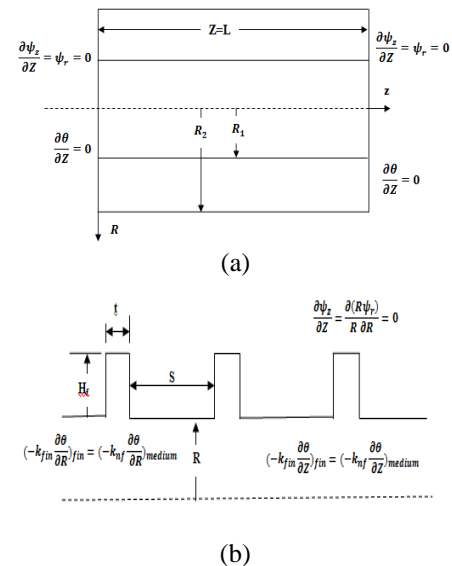$$C_1 = \frac{\alpha_f}{\alpha_{nf}}\left[(1-\varphi) + \varphi\frac{(\rho\beta)_s}{(\rho\beta)_f}\right](1-\varphi)^{2.5} \tag{7}$$

And the energy equation will be:

$$\left(\frac{1}{R}\frac{\partial\psi_z}{\partial\phi} - \frac{\partial\psi_\phi}{\partial Z}\right)\frac{\partial\theta}{\partial R} + \frac{1}{R}\left(\frac{\partial\psi_r}{\partial Z} - \frac{\partial\psi_z}{\partial R}\right)\frac{\partial\theta}{\partial\phi}$$
$$+ \left(\frac{\psi_\phi}{R} + \frac{\partial\psi_\phi}{\partial R} - \frac{1}{R}\frac{\partial\psi_r}{\partial\phi}\right)\frac{\partial\theta}{\partial Z} \tag{8}$$
$$= \frac{\alpha_{nf}}{\alpha_f\ r_2}\left[\frac{\partial^2\theta}{\partial R^2} + \frac{1}{R}\frac{\partial\theta}{\partial R} + \frac{1}{R^2}\frac{\partial^2\theta}{\partial\phi^2} + \frac{\partial^2\theta}{\partial Z^2}\right]$$

And fin equation will be [19]:

$$\frac{\partial\theta}{\partial R} + \frac{\theta}{R} + \frac{1}{R}\frac{\partial\theta}{\partial\phi} + \frac{\partial\theta}{\partial Z} = 0 \tag{9}$$

For the vector potential field, the boundary conditions are given in **Fig. 1**.


(a)

(b)

Figure 1: (a) Annulus boundary conditions (b) Fins boundary conditions

## 4. Computational Technique

The equations were transformed into the finite difference approximation, where the upwind differential method in the left hand side of the energy equation and the centered – space differential method for the other terms were used, and solved by using (SOR) method.

A computer program was built using MATLAB to meet the requirements of the problem. The value of the vector potential ψ calculated at each node, in which the value of vector potential is unknown, the other node will appear in the right hand side of each equation.

The **Fig. 2** illustrate the influence of number of grid points for a test case of $Ra^* = 500$, a=0.8, η=0.01and φ =0.3. The figure shows the average Nusselt number for point located on the inner hot cylinder. The number of grid points used was 21 grid points in the R – direction, 31 in the ϕ – direction and 301 in the Z – direction

Paper ID: 15041501

2142
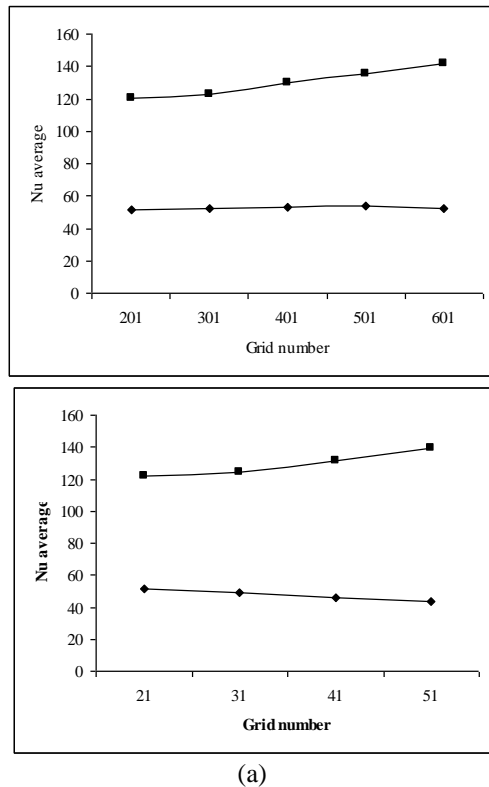
(a)
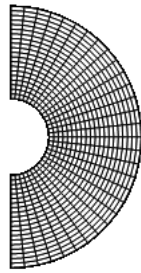
(b)

Figure 2: (a) Grid Size Study at the inner hot cylinder along the length and in R direction (b) grid generation in the Ø direction

5. Hydraulic and Thermal Boundary Conditions

5.1 Dimensionless Hydraulic Boundary Conditions:

$$\frac{1}{R}\frac{\partial}{\partial R}(R\psi) = 0 \qquad at\ R = R_1, 1$$

$$\frac{\partial \psi}{\partial Z} = 0 \qquad at\ Z = 0,\ L$$

And for the fin, the boundary conditions are given as:

$$\frac{1}{R}\frac{\partial}{\partial R}(R\ \psi_r) = \frac{\partial\ \psi_Z}{\partial\ Z} = 0$$

On the fin faces which were located on the following planes:
At R = R₁ for (fin base)

At r = r_in+H_f for (fin tip)

5.2. Dimensionless Thermal Boundary Conditions:

$$\theta = 0 \qquad at\ R = R_2 = 1$$

Case 1: Constant wall temperature

$$\theta = 1 \qquad at\ R = R_1 = r_{in}/r_{out}$$

Case 2: Sinusoidal wall temperature

$$\theta = 1 + a\ \sin(2\pi\ \tau'/\eta') \qquad at\ R = R_1 = r_{in}/r_{out}$$

$$\frac{\partial \theta}{\partial Z} = 0 \qquad at\ Z = 0,\ L$$

At R=H₁

$$-k_{fin}\frac{\partial \theta}{\partial R}\Big|_{fin} = -k_{nf}\frac{\partial \theta}{\partial R}\Big|_{nf}$$

6. Calculation of the Local and Average Nusselt Number

The local Nusselt number Nu_1 and Nu_2 on the inner and the outer cylinders are written in the form:

$$Nu_1 = -(1-R_1)\frac{k_{nf}}{k_f}\left(\frac{\partial \theta}{\partial R}\right)_{R=R_1} \tag{10}$$

$$Nu_2 = -(1-R_1)\frac{k_{nf}}{k_f}\left(\frac{\partial \theta}{\partial R}\right)_{R=1_1} \tag{11}$$

The average Nusselt number Nu_{in} and Nu_{out} on the inner and the outer cylinders are defined as:

$$Nu_{in} = -(1-R_1)\frac{1}{\pi L}\int_0^L\int_0^\pi\left(\frac{\partial \theta}{\partial R}\right)_{R=R}d\phi\ dZ \tag{12}$$

$$Nu_{out} = -(1-R_1)\frac{1}{\pi L}\int_0^L\int_0^\pi\left(\frac{\partial \theta}{\partial R}\right)_{R=1}d\phi\ dZ \tag{6.4}$$

The effect of the nanofluids on heat transfer rate introduced as a variable called Nusselt number ratio (NUR) with its definition given as:

$$NUR = \frac{Nu_{out}\,|_{nanofluid}}{Nu_{out}\,|_{pure\ fluid}} \tag{13}$$

A correlation for Nu in terms of Ra, φ and dimensionless amplitude (a) has been developed for inner hot cylinder as follow:

$$Nu = 13.07\ (Ra^*)^{0.4304}\ \varphi^{0.533}\ a^{0.4003}$$

At S₁ for any R and S₂ for any R

$$-k_{fin}\frac{\partial \theta}{\partial Z}\Big|_{fin} = -k_{nf}\frac{\partial \theta}{\partial Z}\Big|_{nf}$$

7. Results and Discussion

7.1. Temperature, Streamlines and Velocity Fields

The dimensionless temperature distribution and the axial velocity within the enclosure are presented in a contour map form. For isotherms, one section was selected in the (Z-R) plane along the length of the annulus, and the other in the (R-φ) plane, in a manner allowed studying the temperature distribution and streamlines within each plane. For comparison purposes, parameters are selected of constant wall temperature, Ra*=500 and φ=0 in the **Fig. 3** and φ=0.3

in the **Fig. 4**. The **Fig. 3** shows the temperature distribution for pure fluid where the isotherms shift towards the outer (cold) cylinder and a thicker cold layer in the lower region of the annulus wall exist while a high temperature exist in the upper half of the annulus where the waviness in temperature distribution is due to the existence of the fins**.** The figure **Fig.4** illustrates the enhancement in heat transfer where the temperature decrease clearly in the regions between fins. For the streamlines it can be seen from figures that one vortex occur which indicates that the heated flow moves up from the inner heated cylinder of the enclosure and impinges to the cold outer cylinder. The difference between nanofluid and pure fluid cases are the higher intensity of streamlines in nanofluid. The velocity field shows a clear decrease in the axial velocity due to the enhancement in heat transfer caused the fluid to be cooled and as a result the velocity decreased.
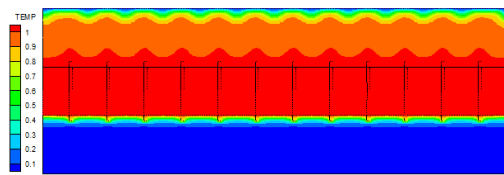
a. Isotherms along annulus length
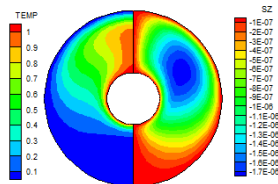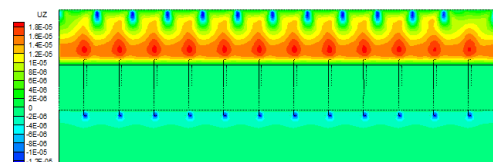

b. isotherms (left), streamlines (right)
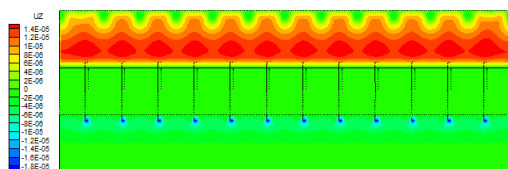
c. Axial velocity along annulus length
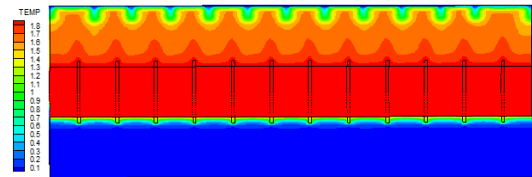**Figure 3:** Ra=500, a=0 and φ=0
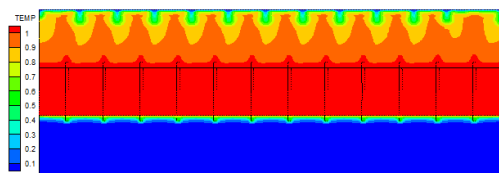
a. Isotherms along annulus length
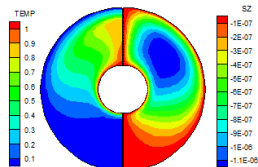
b. isotherms (left), streamlines (right)
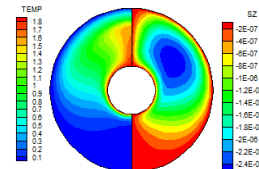

c. Axial velocity along annulus length
Figure 4: Ra=500, a=0 and φ=0. 3

For sinusoidal oscillation in the inner cylinder wall temperature, a selected case is taken for dimensionless amplitude a= 0.8, η=0.01, Ra*=500, φ=0 in the **Fig. 5** and φ=0.3 in the **Fig. 6**.

The **Fig. 5** shows the temperature distribution for pure fluid and that the increase in amplitude cause to enhance heat transfer so the values of isotherms decrease and a decrease in the axial velocity and streamlines intensity observed. In the **Fig. 6** as φ increase to 0.3 an extra enhancement in heat transfer obtained and the enclosure cooled with more decrease in the velocity and streamlines intensity.
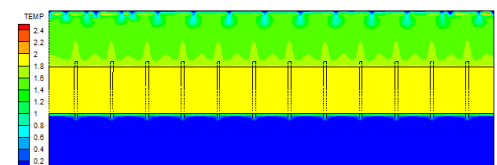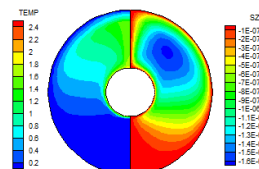

a. Isotherms along annulus length
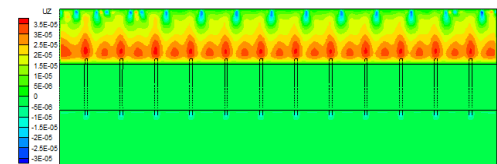

b. isotherms (left), streamlines (right)
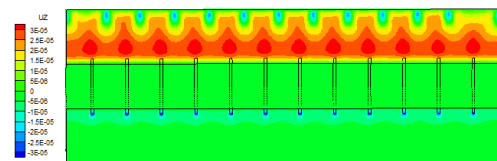
c. Axial velocity along annulus length
**Figure 5:** Ra=500, a=0.8, η=0.01 and φ=0

a. Isotherms along annulus length


b. isotherms (left), streamlines (right)

c. Axial velocity along annulus length
Figure 6: Ra=500, a=0.8, η=0.01 and φ=0. 3

The **Fig. 7** and **Fig. 8** illustrate the variation of Local Nusselt number along the length of the inner cylinder. It is clear from

Paper ID: 15041501

2144

these figures, as mentioned previously that heat transfer enhances by sinusoidal oscillation boundary condition and adding nano particles to the pure fluid causes extra enhancement in heat transfer.


(a) φ = 0

(b) φ = 0.3
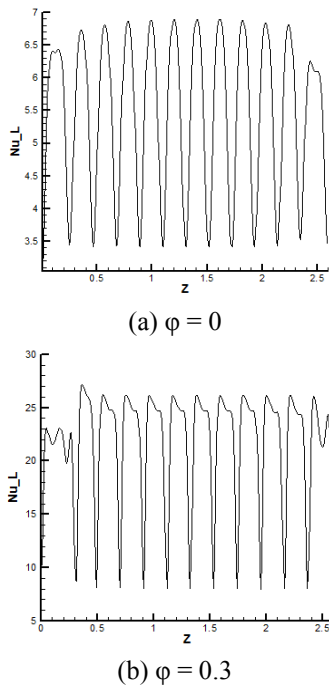
Figure 7: The variation of Local Nusselt number along the length of the inner cylinder for $Ra^*=500$ and for constant wall temperature boundary condition (a=0)


(a) φ = 0

(b) φ = 0.3
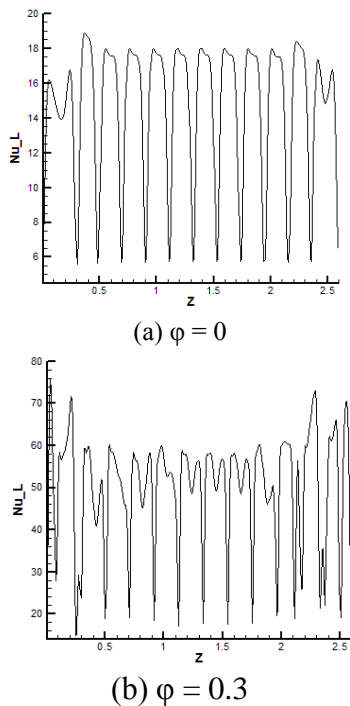
Figure 8: The variation of Local Nusselt number along the length of the inner cylinder for $Ra^*=500$ and sinusoidal oscillation temperature boundary condition (a=0.8)

The variation of the average Nu with the modified Rayleigh number for various volume fractions (φ) and with various wall temperatures boundary condition is illustrated in the **Fig. 9**. This figure shows that for $Ra^*=10$, as the volume fraction increase from zero to 0.3 the enhancement percent

in heat transfer is 1.327% for constant wall temperature and 1.42% for sinusoidal oscillation boundary condition for amplitude equal 0.8.
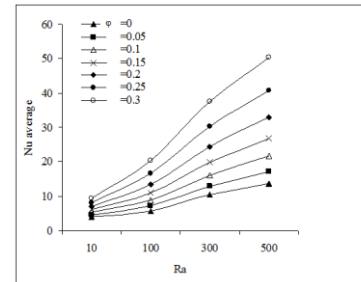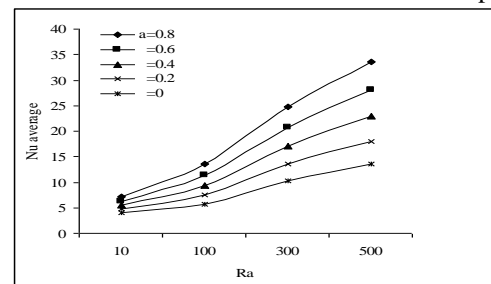

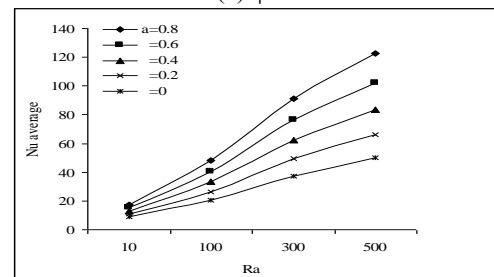(a) Dimensionless amplitude (a) =0
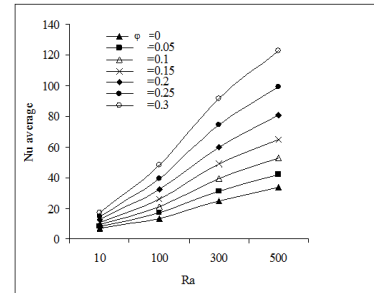
(b) Dimensionless amplitude (a) =0.8

Figure 9: The variation of the average Nu with the modified Rayleigh number for various volume fractions (φ)

The **Fig. 10** shows the variation of the average Nu with the modified Rayleigh number for various dimensionless amplitudes in pure fluid and in nanofluid with volume fraction φ = 0.3. For constant wall temperature with $Ra^*=10$, as the dimensionless amplitude increase from zero to 0.8 the enhancement percent in heat transfer is 0.78 % where in nanofluid with φ=0.3 the enhancement percent is 0.857 %.

The variation of the average Nusselt number with the dimensionless period $\acute{η}$ for dimensionless amplitude a=0.8 and $Ra^*=300$ is shown in the **Fig. 11**; where it is clear that Nu decrease with the increase of the dimensionless period $\acute{η}$.
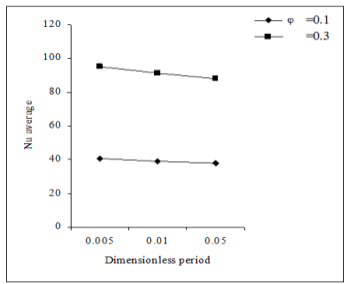

(a) φ =0
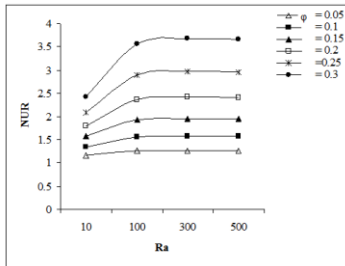

(b) φ =0.3

Figure 10: The variation of the average Nu with the modified Rayleigh number for various dimensionless amplitudes (a)
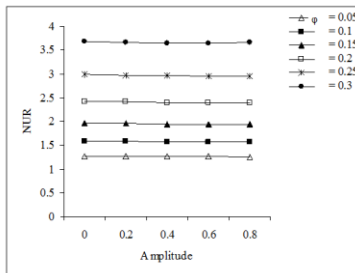
Figure 11: The variation of the average Nusselt number with the dimensionless period $\acute{\eta}$ for dimensionless amplitude a=0.8 and Ra*=300

The **Fig. 12** shows that the Nusselt number ratio (NUR) increase with the modified Rayleigh number increase until Ra* equal about 100 and then the values (for various volume fractions (φ) and a=0.8) reach a steady state. In the **Fig. 13** the variation of the Nusselt number ratio with the dimensionless amplitude (a) for various volume fractions (φ) and Ra*=500 is illustrated and it is clear that NUR is nearly constant with the dimensionless amplitude and increase when adding more copper particles.

Figure 12: The variation of the Nusselt number ratio with the modified Rayleigh number for various volume fractions (φ) and a=0.8

Figure 13: The variation of the Nusselt number ratio with the dimensionless amplitude (a) for various volume fractions (φ) and Ra*=500

8. Conclusion

From the present work results and for the annulus that described previously, the following conclusions can be obtained:

1) The increase in the dimensionless amplitude cause to enhance heat transfer which causes the values of the isotherms to decrease and as consequent a decrease in the axial velocity values and the streamlines intensity observed.
2) Adding copper particles to the pure fluid cause an extra enhancement in heat transfer and the enclosure cooled with more decrease in the velocity and streamlines intensity.

3) For Ra*=10, as the volume fraction increase from zero to 0.3 the enhancement percent in heat transfer is 1.327% for constant wall temperature and 1.42% for sinusoidal oscillation boundary condition.
4) For constant wall temperature with Ra*=10, as the dimensionless amplitude increase from zero to 0.8 the enhancement percent in heat transfer is 0.78 % where in nanofluid the enhancement percent is 0.857 %.
5) For Ra*=500; adding Cu nanoparticles with φ= 0.3 cause 268.18% enhancement in heat transfer. It is found that applying sinusoidal temperature boundary condition causes 1.7% increase in heat transfer than that of constant wall temperature.
6) As Ra* increase, the Nusselt number ratio (NUR) increase until Ra* equal about 100 where it reaches a constant value.

References

[1] Y. C. Ching Soret, Dufour , "Effects on heat and mass transfer by natural convection from a vertical truncated cone in a fluid-saturated porous medium with variable wall temperature and concentration", International Communications in Heat and Mass Transfer vol. 37, pp.1031–1035, 2010.
[2] S.U.S Choi., "Enhancing thermal conductivity of fluids with nanoparticles", ASME Fluids Eng. Div. vol. 231, pp.99–105, 1995.
[3] M. Esmaeilpour, M. Abdollahzadeh, "Free convection and entropy generation of nanofluid inside an enclosure with different patterns of vertical wavy walls", International Journal of Thermal Science vol. 52, pp. 127-136, 2012.
[4] K. Fukuda, Y. Takata, S. Hasegawa, H. Shimomura, K. Sanokawa, "Three – Dimensional Natural Convection in a Porous Medium Between Concentric Inclined Cylinders", Proc. 19th Natl Heat Transfer Conf., Vol. HTD – 8, pp. 97– 103, 1980.
[5] B. Ghasemi, S.M. Aminossadati, "Periodic natural convection in a nanofluid-filled enclosure with oscillating heat flux", International Journal of Thermal Sciences vol. 49, pp. 1–9, 2010.
[6] F. O. Hakan, A.N. Eiyad, "Numerical study of natural convection in partially heated rectangular enclosures filled with nanofluids", International Journal of Heat and Fluid Flow, vol.29, pp. 1326–1336, 2008.
[7] R.Y. Jou, S.C. Tzeng, "Numerical research of nature convective heat transfer enhancement filled with nanofluids in rectangular enclosures", Int. Comm. Heat Mass Transfer, vol.33, No. 6, pp. 727–736, 2006.
[8] K. Khanafer, K. Vafai, M. Lightstone, "Buoyancy-driven heat transfer enhancement in a two-dimensional enclosure utilizing nanofluids", Int. J. Heat Mass Transf. vol. 46, No.19, pp.3639–3653, 2003.
[9] C. L. Kuang, A. Violi, "Natural convection heat transfer of nanofluids in a vertical cavity: Effects of non-uniform particle diameter and temperature on thermal conductivity", International Journal of Heat and Fluid Flow vol. 31, pp.236–245, 2010.
[10] H. S. Kwak, J.M. Hyun, "Natural convection in an enclosure having a vertical sidewall with time-varying temperature", J. Fluid Mech. Vol. 329, pp. 65–88, 1996.

[11] H.S. Kwak, K. Kuwahara, H. Jae Min, "Resonant enhancement of natural convection heat transfer in a square enclosure", Int. J. Heat Mass Transfer. Vol. 41, No. 18, pp.2837–2846, 1998.

[12] J. L. Lage, A. Bejan, "The resonance of natural convection in an enclosure heated periodically from the side", Int. J. Heat Mass Transfer. Vol. 36, No. 8, pp. 2027–2038, 1993.

[13] S.Mina, H. M. Amir, T. Farhad, "A numerical investigation of conjugated-natural convection heat transfer enhancement of a nanofluid in an annular tube driven by inner heat gene rating solid cylinder", Int. communication of Heat and Mass Transfer, vol. 38, pp.533 – 542, 2011.

[14] N. Mohammadreza, S. Ebrahim, H. R. Mohammad, "Investigation of heat transfer enhancement in an enclosure filled with nanofluids using multiple relaxation time lattice Boltzmann modeling", International Communications in Heat and Mass Transfer, vol. 38, pp.128–138, 2011.

[15] M. Mostafa, M. H. Seyed, "Numerical study of natural convection of a nanofluid in C-shaped enclosures", International Journal of Thermal Sciences, vol. 55, pp. 76-89, 2012.

[16] R. Nazar, L. Tham, I. Pop, D. B. Ingham, "Mixed Convection Boundary Layer Flow from a Horizontal Circular Cylinder Embedded in a Porous Medium Filled with a Nanofluid", Trans. Porous Med pp. 86:517–536, 2011.

[17] A.G.A. Nnanna, "Experimental model of temperature-driven nanofluid", J. Heat Transfer, vol.129, No. 6, pp. 697–704, 2007.

[18] Ramón L. F. and Sergio G. M., 2007, Three Dimensional Natural Convection in Finned Cubical Enclosure, Int. J. of Heat and Fluid flow, vol. 28, PP. 289-298.

[19] B. X. Wang, X. Zhang, "Natural Convection in Liquid Saturated Porous Media Between Concentric Inclined Cylinders", Int. J. Heat and Mass Transfer vol. 33. No 5, pp.827-833, 1990.

Author Profile

Manal AL-Hafidh: received the B.S. in 1981 from Mosul University and the M.Sc. and the PhD. degrees in the Mechanical Engineering College from University of Baghdad in 1987 and 2011, respectively. From 1987 until now she is a faculty in the mechanical department. She is specialized in thermo heat, porous media and nanofluids.